HHS Public Access

Author manuscript

J Mol Biol. Author manuscript; available in PMC 2024 December 15.

Published in final edited form as:

J Mol Biol. 2023 December 15; 435(24): . doi:10.1016/j.jmb.2023.168333.

Identification of RBM46 as a novel APOBEC1 cofactor for C-to-U RNA-editing activity

Shanshan Wang[1], **Kyumin Kim**[1], **Nicolas Gelvez**[1], **Claire Chung**[2], **Jean-Francois Gout**[3], **Benjamin Fixman**[4], **Marc Vermulst**[2], **Xiaojiang S. Chen**[1,4,5,6,*]

[1]Molecular and Computational Biology Section, University of Southern California, Los Angeles, CA 90089, USA;

[2]School of Gerontology, University of Southern California, Los Angeles, CA 90089, USA;

[3]Department of Biological Sciences, Mississippi State University, Mississippi State, MS 39762, USA;

[4]Programs in Biomedical and Biological Sciences (PIBBS), Keck School of Medicine, University of Southern California, Los Angeles, CA 90089, USA;

[5]Center of Excellence in NanoBiophysic, University of Southern California, Los Angeles, CA 90089, USA;

[6]Norris Comprehensive Cancer Center; University of Southern California, Los Angeles, CA 90089, USA.

Abstract

Cytidine (C) to Uridine (U) RNA editing is a post-transcription modification that is involved in diverse biological processes. APOBEC1 (A1) catalyzes the conversion of C-to-U in RNA, which is important in regulating cholesterol metabolism through its editing activity on ApoB mRNA. However, A1 requires a cofactor to form an “editosome” for RNA editing activity. A1CF and RBM47, both RNA-binding proteins, have been identified as cofactors that pair with A1 to form editosomes and edit ApoB mRNA and other cellular RNAs. SYNCRIP is another RNA-binding protein that has been reported as a potential regulator of A1, although it is not directly involved in A1 RNA editing activity. Here, we describe the identification and characterization of a novel cofactor, RBM46 (RNA-Binding-Motif-protein-46), that can facilitate A1 to perform C-to-U editing on ApoB mRNA. Additionally, using the low-error circular RNA sequencing technique, we identified novel cellular RNA targets for the A1/RBM46 editosome. Our findings provide further

*To whom correspondence should be addressed. Tel: +1 213 740-5487; FAX: +1 213 740 4340; xiaojiac@usc.edu.

AUTHOR CONTRIBUTIONS

K. Kim. S. Wang and X.S.C designed the conceptual framework for this study. S. Wang, with the assistance of K. Kim, N. Gelvez, B. Fixman, and C. Chung, performed the experiments. S. Wang analyzed the experimental data and J.F. Gout analyzed the sequencing data. S. Wang wrote the initial manuscript draft. K. Kim, M. Vermulst, and X.S.C. revised the manuscript. All co-authors commented on the manuscript.

COMPETING INTEREST

The authors declare no competing interests.

insight into the complex regulatory network of RNA editing and the potential new function of A1 with its cofactors.

Graphical abstract

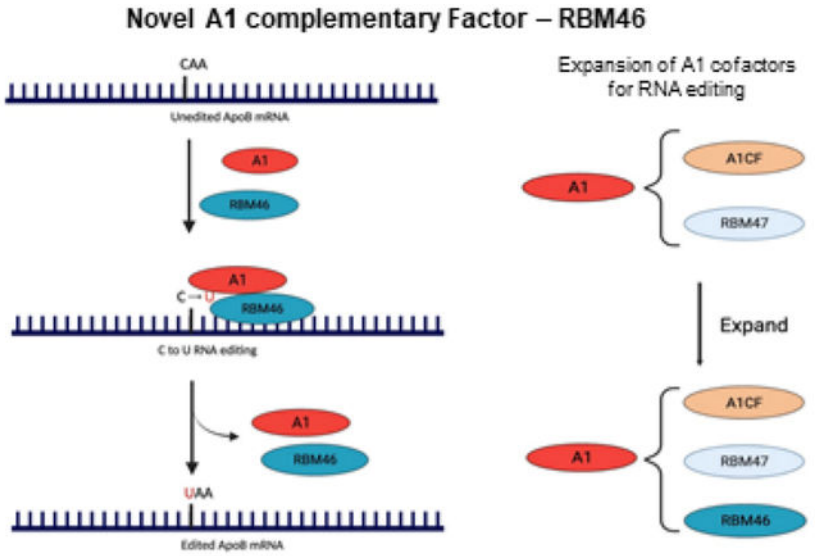

Introduction

The APOBEC deaminase family plays a crucial role in a diverse array of biological functions by catalyzing the conversion of Cytidine (C) to Uridine (U) on RNA and/or DNA [1–3]. The first instance of C-to-U RNA editing was documented in the ApoB mRNA at position 6666, leading to the creation of an early stop codon and the production of two distinct ApoB protein isoforms: ApoB100 and ApoB48, which are implicated in lipid and cholesterol metabolism [4–7]. This RNA editing event is observed in the small intestine of humans and in both the small intestine and liver of mice [8]. APOBEC1 (A1) is responsible for this ApoB RNA editing. A1 requires a cofactor to form a so-called “editosome” complex to show obviously detectible RNA editing activity. The first cofactor identified is called A1 complement factor (A1CF), which is shown to interact with A1 and regulate lipid uptake and metabolism [9–11]. A second cofactor, RNA-Binding-Motif-protein-47 (RBM47), has later been identified to enable A1 RNA editing [12–15]. The possibility of the existence of other RNA binding protein cofactors for A1 has been proposed [16]. Both A1CF and RBM47 contain conserved RNA-recognition motifs (RRM) that directly interact with RNAs [17]. These proteins are conserved across multiple species and are involved in various biological functions [18–20]. While A1CF and RBM47 are homologous proteins and share many RNA substrates for A1 editing, they also showed different substrate specificity and editing efficiency when paired with A1 in both *in vitro* and *in vivo* studies [15, 21].

In addition to A1CF and RBM47, another homologous RNA binding protein called SYNCRIP (Synaptotagmin Binding Cytoplasmic RNA Interacting Protein) is reported to inhibit A1-mediated ApoB RNA editing possibly by binding to and sequestering A1CF, A1, or ApoB RNA [22]. This finding suggests that the A1-mediated RNA editing activities

may be regulated by more cellular cofactors in different ways than previously anticipated. In addition to ApoB RNA, A1 and cofactors are shown in recent years to edit some other cellular RNAs in different types of cells [23–26], indicating that A1-mediated RNA editing may have a much broader range of yet-to-be-characterized biological functions.

In this study, we have identified RBM46 (RNA-binding-motif-protein-46) as a novel cofactor of A1 for RNA editing and have characterized its essential functional domains for enabling A1 to perform RNA editing activity. Using the low-error circular RNA seq technique [27], we have also identified cellular RNA substrates for A1/RBM46 editosome, and have characterized the critical RNA sequence features as the preferred substrate for A1/RBM46 and other A1 editosomes. The identification of RBM46 as a cofactor for A1-mediated RNA editing expands our understanding of the A1-mediated RNA editing mechanism and provides new insights into the biological functions of A1 and its cofactors.

Result

RBM46 is a bone-fide A1 complimentary factor that mediates C-to-U editing

To identify new A1 complementary cofactors for its RNA editing activity, we performed protein-protein BLAST using A1CF and RBM47 sequences. The BLAST result of this analysis showed that, SYNCRIP and RBM46 share a relatively high homology. The homology of RBM46 isoform 1 for the first 406 residues shows more than 70% sequence identity with RBM47, and 68% sequence identity with A1CF (Suppl. Table 1). SYNCRIP has been previously reported as a negative regulator of A1 for RNA editing, but its exact role is not well understood. Here we investigated the function of both RBM46 isoform 1 and SYNCRIP in assisting A1 RNA editing using our previously described cell-based RNA editing assay system [21, 28].

In this cell-based assay system, an editing vector and a reporter vector were co-transfected into HEK293T cell. The editing vector contains human A1 and a potential cofactor (RBM46 or SYNCRIP) (Fig. 1A), in which A1, eGFP, RBM46 or SYNCRIP, and mCherry are all translated within a single open reading frame. The editing vector also contains the self-cutting 2A peptide between A1 and RBM46/SYNCRIP, which produces individual A1 and RBM46/SYNCRIP in a 1:1 ratio [21, 29]. The reporter vector contains a 48-nt ApoB RNA fragment containing editing the A1/cofactor site located downstream of the eGFP coding sequence (Fig. 1A). An AAV intron was inserted into the middle of eGFP to identify mature mRNA transcripts with the intron spliced out and differentiate from the DNA coding for the unspliced RNA containing introns. The protein expression in the HEK293T cells after transfection is examined by Western blot (Sup. Fig. 1A). After cDNA synthesis from the purified RNA extracted from the cells transfected with both the editor and reporter constructs, a primer that anneals to the exon-exon junction on the mature mRNA is used to amplify the ApoB RNA by PCR, ruling out the direct C-to-U mutation on the DNA by A1 (Fig. 1A). The amplified ApoB RNA was subjected to Sanger Sequencing to examine the C-to-U editing by A1 paired with RBM46 or SYNCRIP in the transfected cells. The Sanger Sequencing chromatogram clearly revealed that A1+RBM46 pair showed C-to-U editing activity, with ~65% editing rate on the target C site, but A1+SYNCRIP pair did not show C-to-U editing on the site (Fig. 1B–C). As controls, A1, RBM46, or SYNCRIP alone did not

show C-to-U editing on the target C site, and A1+A1CF or A1+RBM47 showed over 75% or 90% editing rates, respectively (Fig. 1B–C).

To validate the results from the cell-based assay system, a primer extension assay [30] was also applied to examine the *in vitro* editing activity of purified proteins of A1 paired with RBM46 and in parallel with A1CF, RBM47, and SYNCRIP. Consistent with the Sanger Sequencing result, the presence of ApoB RNA alone or individual A1, A1CF, RBM47, RBM46, or SYNCRIP does not show detectible editing on ApoB RNA, whereas A1 paired with RBM46, A1CF, or RBM47 all showed RNA editing (Fig. 1D). This result suggests that RBM46 is a bone-fide cofactor (or complementary factor) to facilitate A1's RNA editing activity on ApoB RNA, while SYNCRIP cannot facilitate A1 RNA editing.

Comparing the editing rate of RBM46 with other known A1-cofactors on different RNAs

Previous reports showed that RBM47 and A1CF can complement A1 to edit many other RNA substrates with different editing efficiency [21, 23, 31, 32]. We want to compare the editing rate of A1+RBM46 with A1 plus other known cofactors on a few previously reported RNA substrates using the cell-based assay system. Various reporter constructs were generated to contain an insertion of a 48-nt RNA segment of the eight known RNA targets from mice genes as described previously for the cell-based RNA-editing assay [21], and those RNA targets were previously shown to be edited by human A1 and A1CF/RBM47 cofactors [21, 23, 32].

The results of these editing assays of A1 paired with its different cofactors (RBM46, A1CF, RBM47, and SYNCRIP) are summarized in Fig 2A–B. The data illustrates that when A1 is paired with RBM46, there is a notable increase above the background levels in editing activity for ApoB, Ptpn3, and Fmn1. Conversely, no significant increase in editing activity above the background was observed when A1 was paired with SYNCRIP. However, A1 paired with different cofactors showed different editing rates on different substrates. ApoB RNA, Ptpn3, Fmn1, and Usp25 RNA showed the highest editing with cofactor RBM47, and the lowest editing activity with RBM46. Serinc1 RNA showed a similar editing level with A1CF or RBM47, but no editing with RBM46. Dpyd RNA only showed a low level of editing with A1CF. Cd36 and Sh3bgrl RNA showed some level of editing with RBM47, and Sh3bgrl RNA also showed a lower level of editing with A1CF. Csp6 RNA displayed a low level of editing with A1CF, RBM47, and RBM46, but a little higher level of editing with RBM47. Those data suggest that the editing efficiency on these different substrates by A1 is regulated by different cofactors.

To examine whether the sequence outside the 48-nt segment of the target RNA will significantly impact the secondary structure of the target RNA and editing efficiency, we compared the editing rate of a 96-nt RNA fragment with thee 48-nt fragment in the containing ApoB_RNA and Ptpn3_RNA (Fig. 2C). The results in Fig. 2D showed that ApoB-96nt RNA substrate showed a significantly higher editing level than ApoB-48nt RNA with cofactor RBM46 and A1CF, and a similar editing level with RBM47. Ptpn3-96nt RNA showed a significantly higher editing level than Ptpn3-48nt RNA with all three cofactors. In addition, ApoB-96nt RNA also showed a significantly higher editing level by A1 alone and A1 paired with SYNCRIP, and the editing activity might be cofactor independent or

A1 is paired with other yet to be identified protein co-factors [33]. Those data confirm that previously known RNA candidates of A1 and A1CF/RBM47 can be also edited by A1 and its novel cofactor, RBM46, and that the length of the tested RNA segment between 48-nt and 96-nt can affect the editing efficiency in a quantitative manner for some substrates.

RBM46 domains essential for complement A1 RNA editing activity

Several studies have already characterized the A1/A1CF and A1/RBM47 interaction and determined the minimal functional domains of A1CF and RBM47 required for facilitating A1 RNA editing [14, 21, 34, 35]. RBM46 is a 533 amino acid RNA binding protein that contains 3 RNA-recognition-motif (RRM 1–3) (Fig. 3A). The RRM is highly conserved in a large family of RNA binding proteins, including A1CF and RBM47 [17]. To characterize the domain of RBM46 required to complement A1 RNA editing, a series of C-terminal deletions of the full-length RBM46 in the editor construct were generated (Fig. 3B) for the cell-based editing assay. The results showed that no editing activity was observed when A1 was paired with the two shortest C-terminal deletions of RBM46 1–281 and 1–306 (Fig. 3C). A1 paired with RBM46 1–341 and 1–369 showed a partial editing activity (Fig. 3C). Almost full editing activity can be achieved when A1 paired with other longer RBM46 constructs with shorter C-terminal deletions (Fig. 3C). Those results indicate that RBM46 domain between amino acid 281 and 341 are essential, and this domain contains RRM3.

To investigate whether the physical interactions of A1 with RBM46 depend on RBM46 domain between amino acid 281 and 341, FLAG-tagged A1 was co-transfected with HA-tagged RBM46 with deletion of amino acid 281 to 341 into HEK293T cells. Co-immunoprecipitation followed by Western blot analysis was used to examine the interactions. The co-immunoprecipitation was performed with or without RNase A treatment of the cell lysate to evaluate the RNA contribution to the physical interactions. The results showed that FLAG A1 interacted with RBM46 missing amino acid 281–341 with or without RNase A treatment (Fig. 3D), suggesting that the interactions of A1 with RBM46 are not dependent on RBM46 domain between amino acid 281–341.

To assess the significance of each individual RRM domain in A1 RNA editing, we created variants of the RBM46 editor construct, each lacking one or more of the RRM domains (RRM1, RRM2, RRM3, or both RRM1 and RRM2). We then conducted a cell-based editing assay on ApoB RNA. Our findings revealed that the absence of the RRM1 domain in RBM46 resulted in an editing level comparable to the full-length RBM46 (Fig. 3E). In contrast, when RRM2, RRM3 (amino acids 281–341 of RBM46), or both RRM1 and RRM2 were removed, there was no discernible editing activity above the baseline (Fig. 3E). This suggests that while the RRM1 domain is not crucial, both RRM2 and RRM3 are essential for RBM46's role in enhancing A1 editing of ApoB RNA. Additionally, the C-terminal domain following RRM3 in RBM46 appears to contribute to the A1 editing process on ApoB RNA.

Role of cofactor the three RRMs in facilitating A1 RNA editing activity

The RRMs are highly conserved among the family of RRM-containing RNA binding human gene, which contains 337 annotated human gene [36], including A1CF, RBM47, RBM46,

and SYNCRIP (Suppl. Table 1) [17], and they are critical for facilitating A1 RNA editing activity. However, of these four proteins, only SYNCRIP cannot facilitate A1's RNA editing activity. To better understand the roles of different RRMs in their ability to complement A1 activity, we constructed SYNCRIP chimeras with its three RRMs replaced with the RRMs from RBM46 and RBM47 (Fig. 4B–C) and test their ability to complement A1 activity in the cell-based assay system.

The results revealed that the SYNCRIP chimeras with all its three RRMs replaced with those of RBM47 (SYNCRIP_RBM47-R1R2R3) or RBM46 (SYNCRIP_RBM46-R1R2R3) displayed RNA editing activity comparable to that with RBM47 or with RBM46 (Fig. 4C–D). These results suggest that it is the three RRM domains that are critical domains for facilitating the A1-mediated RNA editing activity for ApoB RNA. The result also indicates that the SYNCRIP chimeras with the replacement of only one or two RRMs from RBM47 and RBM46 also showed some level of RNA editing on ApoB RNA. A1 paired with SYNCRIP_RBM47-R1R3 showed similar but lower RNA editing activity than when A1 paired with SYNCRIP_RBM46-R2R3 (Fig. 4C–D), indicating that the closely related R2 and R3 of RBM46 and RBM47 have a different effect in complementing A1 RNA editing.

To further confirm the critical role of RRMs for A1-mediated RNA editing, we also generated RBM47 chimeras with its RRMs switched with those of SYNCRIP and examine the RNA editing in the presence of A1. The result showed that the replacement of RBM47 RRM2 by SYNCRIP-RRM2 does not alter the editing activity, suggesting that RBM47 RRM2 may be dispensable. (Sup. Fig. 2). When all three RRMs were replaced with those of SYNCRIP, the RBM47 chimera (RBM47_SYN-R1R2R3) showed only about 10% of the WT RBM47 activity. We showed earlier in Fig. 3E that RBM46-RRM1 is dispensable in A1+RBM46 RNA editing. These results demonstrate that the RRM domains in RBM46 and RBM47 are important in supporting A1 RNA editing activity, and that the three RRM domains of RBM46 and RBM47 and SYNCRIP may serve distinct functions.

Subcellular localization and interaction of A1 and RBM46

A previous study reported that RBM47 and A1CF co-localize and interacts with A1 in cells [14]. We investigated the subcellular localization of RBM46 alone and in the presence of A1 overexpression. A1-eGFP or A1 cofactor-mCherry (RBM46, together with A1CF, RBM47, and SYNCRIP) constructs were transfected in HEK293T cells individually or together and their subcellular localization was examined using confocal fluorescence microscopy. The results revealed that, when individually expressed alone, A1CF and SYNCRIP were predominantly localized in the nucleus. A1 appeared to have roughly equal distribution between the nucleus and cytoplasm, and RBM47 showed more abundant in the cytoplasm than in the nucleus, whereas RBM46 was mostly in the cytoplasm (Fig. 5A). When A1-eGFP was co-transfected with a cofactor-mCherry constructs in HEK293T cell, colocalization of A1 with each of the cofactors were observed in the cytosol or nucleus. However, except that the co-expression of A1 and A1CF results in an increase in the nuclear relocalization of A1, no obvious shifting of the localization of A1 or its other cofactors was observed when compared with expression alone. The fluorescent image result did not show strong co-localization in nucleus between A1-eGFP and RBM46-mCherry.

However, the merging of the eGFP and mCherry color suggests some level of co-localization of A1-eGFP with each of the co-expressed cofactors: A1CF-mCherry, RBM47-mCherry, RBM46-mCherry, and SYNCRIP-mCherry (Fig. 5B). When each of the three cofactors was co-transfected with another cofactor (a total of six pairs of cofactors), again no obvious shift of localization was observed for each pair. However, co-localization of RBM46-eGFP with RBM47-mCherry in the nucleus and cytosol suggests some shift of cytosol localized RBM46 to the nucleus might have occurred (Sup. Fig. 3), even though further study would be needed to confirm this observation.

To investigate the physical interactions of A1 with RBM46 and other cofactors, FLAG-tagged A1 was co-transfected with HA-tagged cofactors into HEK293T cells. Co-immunoprecipitation followed by Western blot analysis was used to examine the interactions. Because A1CF, RBM47, RBM46, and SYNCRIP are all RNA-binding proteins, the co-immunoprecipitation was performed with or without RNase A treatment of the cell lysate to evaluate the RNA contribution to the physical interactions. The results showed that FLAG A1 interacted with all four cofactors with or without RNase A treatment, suggesting that the interactions of A1 with these cofactors are not dependent on RNA (Fig 5C). Taken together, these results show that RBM46 co-localizes and interacts with A1 and can serve as a cofactor of the A1 RNA editosome complex.

Identification of novel RNA targets by A1+RBM46 using circular RNAseq

We further investigated potential cellular RNA targets for A1 and RBM46 editosome. The editor plasmid containing A1 and RBM46 was transfected in HEK293T cells. Total RNAs were extracted from the HEK293T cells 48 hours post-transfection and then subjected to a low error circular RNA sequence strategy as described in [27]. Comprehensive RNA sequence comparison between cells over-expressing A1 with RBM46 and cells without to examine A1+RBM46-dependent C-to-U RNA editing. We select an arbitrary cutoff of 30% C-to-U editing for further analysis.

Thirty RNA targets have been identified with sites of over 30% C-to -U editing rate by A1 and RBM46 (Table 1). These targets represent novel RNA substrates that have not been previously reported for A1 editing. To validate the circular RNA sequencing results, we used conventional Sanger Sequencing to analyze six RNA targets selected from the thirty identified RNAs (Table 1), including GMNN, PNRC2, FBXO28, PPM1D, STT3B, and RLF. The editing site in RLF is in the coding region, and the editing activity will result in threonine (ACA) to isoleucine (AUA) mutation. The editing sites in the other five RNA targets are in the 3’UTR region, and the consequence of such editing on the RNA expression, stability, and translation efficiency will require future investigation. Total endogenous RNAs were extracted from HEK293T cells after the over-expression of A1 only and A1 paired with RBM46 and other cofactors A1CF and RBM47, and the cDNAs of these six RNAs were synthesized from the total RNA extraction for Sanger sequencing. The results showed that all six RNA targets were edited not only by A1+RBM46, but also by A1+A1CF and A1+RBM47 (Fig. 6A–B), validating the circular RNA sequence results. When comparing the editing level by A1 with different cofactors on different RNA targets, GMNN, PNRC2, FBXO2, and PPM1D showed much higher editing by A1+RBM46. In

contrast, STT3B and RLF showed a similar level of editing by each of the three A1+ cofactor pairs.

An AAA RNA sequence motif preferred by A1+RBM46

Previous study reported that the ApoB RNA editing by A1 and A1CF required mooring sequence that consists of the high content of U, G, and A located downstream of targeted C [37]. However, this mooring sequence requirement is shown to be more relaxed for A1 with its cofactors [21, 38], and the exact features defining the preferred substrates of A1 and cofactors need further investigation. We also investigate the sequence motif near the target C sites for the RNA targets from Table 1 (n=30). Analysis of the sequence contexts around the identified target AC sites (with ± 10 nucleotides from target C) reveals AU-rich sequence on both sides of the targets, which is in line with the previous report that A1 preferred editing sites within AU-rich 3'-UTR region (Fig. 7A) [23]. Furthermore, the analysis also revealed that the AAA motif (or TTT on the – strand) is predominantly present at the −3, −4, and −5 positions among most of the 30 new RNA targets (Table 1 and Sup. Fig. 4). To verify the significance of the AAA motif at the −3 to −5 positions for A1+RBM46-mediated RNA editing, we selected 4 known RNA targets without AAA motif at the −3 to −5 positions, including ApoB, Serinc1, Fmn1, and Usp25, from Figure 2 [5, 21, 23], for mutational testing. The AAA motif at −3 to −5 positions was added to these RNA target sites by site-direct mutagenesis (ApoB RNA as an example in Fig. 7B) and the editing efficiency on these RNAs by A1 plus RBM46 and other cofactors was examined using the cell-based assay system.

The results showed that A1+RBM46 showed increased editing on all 4 substrates after adding AAA motif to the −3 to −5 positions, and a statistically significant increase of editing on 3 out of the 4 substrates, which include ApoB, Serinc1, and Usp25 (Fig. 7). A1+RBM47 also showed a significant increase of editing on Serinc1 and Usp25, even though the increase is less profound than A1+RBM46. However, A1+A1CF did not show a significant increase in editing on any of the targets after adding the AAA motif. Surprisingly, A1 alone also showed significant increase of editing on ApoB_AAA target, probably because of low endogenous expression of RBM46 or other cofactors in HEK293T cells (Sup. Fig. 5).

We next tested the role for AAA motif using GMNN RNA, a novel RNA target containing the AAA motif identified for A1+RBM46 (Table 1). The original AAA motif in GMNN was mutated to AUA, UUA, and UUU for editing test by A1+RBM46 and A1 plus other cofactors. The results showed that A1+RBM46 edited the original RNA sequence with AAA motif at −3 to −5 positions at much higher rate than A1+A1CF and A1+RBM47 (Sup. Fig. 6). However, the editing rate of A1+RBM46 on the mutated RNA substrate showed a dramatic decrease of editing (about 5–10 fold decrease) on the mutated GMNN RNAs. The AAA motif mutation also reduced editing by A1+RBM47 and A1+A1CF, but with much less profound effect. Together, these results suggest that AAA motif at −3 to −5 positions plays a significant role in enhancing the editing efficiency by A1+RBM46 on most of its RNA targets, but has a less but detectible effect in increasing editing efficiency by A1+RBM47 and A1+A1CF.

Discussion

In this study, we have shown that RBM46 is a novel A1 cofactor that can assist A1 to edit ApoB and a few other known RNA targets of A1 and SYNCRIP played no role in facilitating A1 editing activity. We also characterized the functional domain requirements of RBM46, and the result indicates that the RRM1 domain for RBM46 is dispensable for facilitating A1's RNA editing activity and the C-terminus residue can also enhance the editing activity. The investigation of SYNCRIP-gain-of function through SYNCRIP-chimeras containing the RRMs from RBM46/RBM47 indicates that while RRM domains of each protein share high sequence conservation [17], the difference of amino acids of these RRM domains can have significant differences on their ability to modulate A1-mediated RNA editing. Additional research is necessary to explore the distinctions between SYNCRIP and other cofactors, including differences in RNA-binding and interactions with A1.

The previous study already showed that A1 co-localizes and interacts with A1CF and RBM47 when editing on ApoB RNA [14]. In this study, we showed that A1 also interacts and co-localizes with RBM46 in the HEK293T cells, and the interaction is RNA-independent (Fig. 5). Even though SYNCRIP did not exhibit A1-mediated RNA editing activity on ApoB RNA (Fig. 1), it showed physical interaction with A1 (Fig. 5). Even though A1 plus one of the cofactors is capable of editing RNA, whether a cellular A1 editosome contains more than one cofactor at the same time will need further investigation.

Using a highly accurate circular RNA sequencing technique [27], we have identified thirty new RNA substrates for A1+RBM46. Some of these new targets can also be edited by A1 paired with A1CF or RBM47, implying that A1 has broader cellular RNA substrates and biological functions that have yet to be characterized. Most of these newly identified RNA targets share a AAA motif at −3 to −5 positions (or TTT in the –strand), which has not been previously described. We showed that the AAA motif can increase the editing rate by A1+RBM46, and less so A1+RBM47 or A1CF.

In summary, our study has identified RBM46 as a novel cofactor of A1, which facilitates A1 RNA editing. We characterized the essential domains required for complementing A1's editing activity and determined that the RRMs are critical and RRM1 is dispensable for RBM46 to complement A1. Additionally, we have identified novel cellular RNA targets for A1+RBM46 and characterized the AAA sequence motif preferred by A1+RBM46. By comparing the editing activity of RBM46 with the two other known cofactors on different substrates, we showed that different cofactors have different editing rates on different substrates and have different preferences for a AAA sequence motif upstream of the AC target site, even though the side-by-side comparison of RNA editing target by A1 and different cofactor still need to be further studied through NGS in the future. Furthermore, we found that each of the three RRMs from RBM46 and RBM47 can function to some degree to facilitate A1 editing activity. However, when combining three RRMS, we observed a synergistic effect. To gain a more detailed mechanistic understanding of how these cofactors regulate A1 RNA editing activity, structural information on how these RRM-containing cofactors interact with A1 and RNA will be required.

Method

The cell-based RNA editing system and Sanger Sequencing

The cell-based RNA editing system is adapted from a previously reported study in our lab [21]. Editor vectors containing A1 and cofactors (A1CF, RBM47, RBM46, SYNCRIP) are constructed as one open reading frame (ORF) with a self-cleavage peptide T2A inserted between A1 and cofactors, resulting in individual A1 and cofactors proteins in a 1:1 ratio [21, 29]. Reporter vectors contain 48nt substrates DNA including the target C site (Fig. 1A). HEK293T cells are cultured in DMEM medium containing 10% FBS, streptomycin (100μg/mL), and penicillin (100U/mL) and incubated at 37 °C, 5% CO_2. The cell suspension solution (250μL) was seeded one day before transfection at an approximate concentration of 250,000 cells/mL on an 8-well glass chamber (CellVis). The A1 and cofactor editor vector (500ng) and substrate reporter vector (50ng) in a mixture form (25 μL) are transfected in the HEK293T cells using Lipofectamine 3000 Transfection Reagent (Thermo Fisher) and incubated for 48h, according to the manufacturer's recommended instructions. After harvesting the cell, RNA extraction with Trizol (Thermo Fisher) is performed. The extracted RNA is reverse-transcribed using ProtoScript II reverse transcriptase (NEB) to produce the single-stranded cDNA with specific primer annealing to the downstream sequence of substrate reporter segments. The reaction is performed in a volume of 20μL including 1μg of total RNA, 100 μM of reverse primer, ProtoScript II reverse transcriptase buffer, 10 mM dNTP, 0.1M DTT, 8U RNase inhibitor, and 0.2 μL of ProtoScript II reverse transcriptase (NEB) for 1 hour at 42 °C. Then the cDNA is amplified using Phusion High-Fidelity DNA Polymerase (NEB) for 30 cycles [98 °C 2.5 min - (98 °C 20s, 71.7 °C 20s, 72°C 30s) × 30 – 72°C 5 min] by using a forward primer that anneals to the junction region (JUNC, Fig. 1A), where the AAV intron is sliced out. The PCR product is then cleaned up using a spin column PCR cleanup kit (Thermo Fisher) to remove the free primers. The PCR clean-up product is sent to Genewiz for Sanger Sequencing using junction forward primer.

His8 Tagged Protein Purification

Generally, 2 liters of LB-ampicillin media are inoculated and grown at 37 °C until the log phase, and then 150 μM final concentration of IPTG is added and cultured overnight at 16 °C for induction. Cells are lysed using a shear force fluid homogenizer (Microfluidics, Inc) in a lysis buffer containing 20 mM Tris-HCl, 250 mM NaCl (pH 7.5), and 0.5 mM TCEP. After centrifuging at 13000 rpm for 0.5 hours, the cell lysates are incubated with 2 mL Ni resin for 10min and then passed the Ni resin. Then the Ni resin is washed with three full column volumes of washing buffer (10–50mM imidazole) and the protein is eluted with elution buffer (100–300mM imidazole). The protein is concentrated using centrifugal spin concentrators (Millipore). Concentrated His8-RBM46 and His8-SYNCRIP proteins are further purified by size exclusion chromatography (SEC) in a lysis buffer.

RNA deamination: in vitro poisoned primer extension

In vitro poisoned primer extension assay is adapted from the previous study [4]. Purified recombinant MBP-A1 and cofactors are combined at a 1:1 ratio and allowed to react on the in vitro transcribed ApoB RNA. The reaction buffer contains 20 mM HEPES, pH 7.5, 50 mM NaCl, 5 mM DTT, 1 U/μL of RNAase A, and 1 μM RNA. Then 10 μL reactions are

allowed to incubate at 37 °C overnight, and a 5′-FAM-labeled primer with the 1.2 μM final concentration that binds downstream of the editing site with the sequence 5′-AAT CAT GTA AAT CAT AAC TAT CTT TAA TAT ACT GA-3′ are added. Also, a reverse transcription buffer is then added that results in a final concentration of 2.5 U/μl Protoscript II (NEB), 1× manufacturer-recommended reverse transcription buffer, 5 mM DTT, 250 μM dTTP, dCTP and dATP, and 250 mM ddGTP (Tri-link Bio), and 0.1 U/μl of RNase A. After reverse transcription at 42 °C for 1 h, the products are run on a 20% acrylamide urea denaturing gel and visualized by using Typhoon RGB Biomolecular Imager (GE Healthcare).

Fluorescence confocal microscopy

48 hours after transfection of the editor containing A1 and cofactors, the DMEM media is aspirated, and the cells are washed once with 250μL of PBS. Then the cells are incubated with a 5μg/mL solution of Hoechst 33342 nuclear stain diluted in PBS for 15min. This stain solution is then aspirated, and cells are rinsed by PBS twice and then stored in an imaging buffer containing 140mM NaCl, 2.5mM KCl, 1.8mM $CaCl_2$, 1.0mM $MgCl_2$, 20mM Hepes (pH 7.4), and 5mM glucose. A Zeiss LSM-780 inverted confocal microscope is used for A1 and cofactors localization visualizations through a 40X water-immersion objective. The excitation wavelengths used for Hoechst 33342, eGFP, and mCherry are 405mm, 488mm, and 555mm respectively. Images are captured using multichannel 16-bit grayscale intensity images 1012 $_X$ 1012 pixels across, and two-pass line averaging for smoothing and a pixel dwell time of 0.8μs. For each well, approximately three images are captured. The captured images are opened and analyzed by ImageJ software [39].

Co-immunoprecipitation and Western blot

Each group's cells are seeded on two 6-well plates (CELLTREAT) one day before transfection. The FLAG-tagged A1, HA-tagged cofactor, and FLAG-A1-T2A-HA-Cofactors editor vector (2400ng) are transfected in the HEK293T cells using Lipofectamine 3000 Transfection Reagent (Thermo Fisher) and incubated for 48h. After harvesting the cell, 100μL 1X RIPA lysis buffer (Sigma) is used to lyse the cell for each well to get 90μL cell lysate in each sample. For the cell lysate from one 6-well plate, RNaseA (20μg/mL) is added. 15μL of cell lysate (+/− RNaseA) for each sample is saved for input protein expression check using Western blot. Anti-FLAG® M2 Magnetic Beads (Sigma) are washed with RIPA buffer three times before adding to the cell lysates. The cell lysates containing the Anti-FLAG® M2 Magnetic Beads are incubated at 4°C overnight. The beads are then washed with RIPA buffer 3 times and eluted with 30μL 2X SDS at 90°C for 30min. The lysates are then subjected to Western blot with anti-FLAG M2 mAb (F3165, Sigma, 1:3000), anti-HA mAb (HA.C5, Abcam, 1:3000), and anti- α-tubulin mAb from mouse (GT114, GeneTex, 1:5000) as primary antibodies. Then Cy3-labelled goat-anti-mouse mAb (PA43009, GE Healthcare, 1:3000) is used as a secondary antibody. Cy3 signals are detected and visualized by using Typhoon RGB Biomolecular Imager (GE Healthcare).

Circular RNAseq Method

Cell culture and RNA extraction: HEK293T cells are cultured in DMEM medium containing 10% FBS, streptomycin (100μg/mL), and penicillin (100U/mL) and incubated

at 37 °C, 5% CO_2. The cell suspension solution was seeded one day before transfection at an approximate concentration of 250,000 cells/mL on a 10cm plate (CellVis). The A1 and RBM46 editor vector (24μg) are transfect8ed in the HEK293T cells using Lipofectamine 3000 Transfection Reagent (Thermo Fisher) and incubated for 48h, according to the manufacturer's recommended instructions. After harvesting the cell, RNA extraction using RiboPure™ RNA Purification Kit is performed to enrich mRNA.

Library Construction and Sequencing: Library preparation 1100 ng of enriched mRNA was fragmented with the NEBNext RNase III RNA Fragmentation Module (E6146S) for 25 minutes at 37°C. RNA fragments were then purified with an Oligo Clean & Concentrator kit (D4061) by Zymo Research according to the manufacturer's recommendations, except that the columns were washed twice instead of once. The fragmented RNA was then circularized with RNA ligase 1 in 20 μl reactions (NEB, M0204S) for 2 hours at 25°C after which the circularized RNA was purified with the Oligo Clean & Concentrator kit (D4061) by Zymo Research. The circular RNA templates were then reverse transcribed in a rolling-circle reaction by first incubating the RNA with for 10 minutes at 25°C to allow the random hexamers used for priming to bind to the templates. Then, the reaction was shifted to 42°C for 20 minutes to allow for primer extension and cDNA synthesis. Second strand synthesis and the remaining steps for library preparation were then performed with the NEBNext Ultra RNA Library Prep Kit for Illumina (E7530L) and the NEBNext Multiplex Oligos for Illumina (E7335S, E7500S) according to the manufacturer's protocols. Briefly, cDNA templates were purified with the Oligo Clean & Concentrator kit (D4061) by Zymo Research and incubated with the second strand synthesis kit from NEB (E6111S). Double-stranded DNA was then entered into the end-repair module of RNA Library Prep Kit for Illumina from NEB, and size selected for 500–700 bp inserts using AMPure XP beads. These molecules were then amplified with Q5 PCR enzyme using 11 cycles of PCR, using a two-step protocol with 65°C primer annealing and extension and 95°C melting steps. Sequencing data was converted to industry standard Fastq files using BCL2FASTQv1.8.4.

Error Identification: Tandem repeats are identified within each read (minimum repeat size: 30nt, minimum identity between repeats: 90%), and a consensus sequence of the repeat unit is built. Next, the position that corresponds to the 5' end of the RNA template is identified by searching for the longest continuous mapping region. The consensus sequence is then reorganized to start from the 5' end of the original RNA fragment, mapped against the genome with tophat (version 2.1.0 with bowtie 2.1.0) and all non-perfect hits go through a refining algorithm to search for the location of the 5' end before being mapped again. Finally, every mapped nucleotide is inspected and must pass 5 checks to be retained: 1) it must be part of at least 3 repeats generated from the original RNA template; 2) all repeats must make the same base call; 3) the sum of all qualities scores of this base must be >100; 4) it must be >2 nucleotides away from both ends of the consensus sequence.

Graphing and statistical analysis tools

The sequence logos are created by WebLogo3 online tool with probability units [40]. The editing result graphs are made by Graphpad Prism 9. The two-tailed t-test is also done with the build-in t-test of Graphpad Prism 9.

Supplementary Material

Refer to Web version on PubMed Central for supplementary material.

ACKNOWLEDGEMENT

We acknowledge the support of the Translational Imaging Center at the University of Southern California for providing the fluorescent microscope. This work is supported by the NIH grant R01 AI150524 to X.S.C.

Reference

1. Chen Z, Eggerman TL, and Patterson AP, ApoB mRNA editing is mediated by a coordinated modulation of multiple apoB mRNA editing enzyme components. Am J Physiol Gastrointest Liver Physiol, 2007. 292(1): p. G53–65. [PubMed: 16920700]
2. Salter JD, Bennett RP, and Smith HC, The APOBEC Protein Family: United by Structure, Divergent in Function. Trends Biochem Sci, 2016. 41(7): p. 578–594. [PubMed: 27283515]
3. Saraconi G, et al. , The RNA editing enzyme APOBEC1 induces somatic mutations and a compatible mutational signature is present in esophageal adenocarcinomas. Genome biology, 2014. 15(7): p. 1–10.
4. Driscoll DM, Wynne JK, Wallis SC, and Scott J, An in vitro system for the editing of apolipoprotein B mRNA. Cell, 1989. 58(3): p. 519–25. [PubMed: 2758465]
5. Chen SH, et al. , Apolipoprotein B-48 is the product of a messenger RNA with an organ-specific in-frame stop codon. Science, 1987. 238(4825): p. 363–6. [PubMed: 3659919]
6. Blanc V, et al. , Intestine-specific expression of Apobec-1 rescues apolipoprotein B RNA editing and alters chylomicron production in Apobec1 −/− mice. J Lipid Res, 2012. 53(12): p. 2643–55. [PubMed: 22993231]
7. Powell LM, et al. , A novel form of tissue-specific RNA processing produces apolipoprotein-B48 in intestine. Cell, 1987. 50(6): p. 831–40. [PubMed: 3621347]
8. Teng B, Black DD, and Davidson NO, Apolipoprotein B messenger RNA editing is developmentally regulated in pig small intestine: nucleotide comparison of apolipoprotein B editing regions in five species. Biochem Biophys Res Commun, 1990. 173(1): p. 74–80. [PubMed: 2256939]
9. Hirano K, et al. , Targeted disruption of the mouse apobec-1 gene abolishes apolipoprotein B mRNA editing and eliminates apolipoprotein B48. J Biol Chem, 1996. 271(17): p. 9887–90. [PubMed: 8626621]
10. Teng B, et al. , Effective lowering of plasma, LDL, and esterified cholesterol in LDL receptor-knockout mice by adenovirus-mediated gene delivery of ApoB mRNA editing enzyme (Apobec1). Arterioscler Thromb Vasc Biol, 1997. 17(5): p. 889–97. [PubMed: 9157952]
11. Nakamuta M, et al. , Phenotype Interaction of *apobec-1* and *CETP*, *LDLR*, and *ApoE* Gene Expression in Mice. Arteriosclerosis, Thrombosis, and Vascular Biology, 1998. 18(5): p. 747–755. [PubMed: 9598833]
12. Henderson JO, Blanc V, and Davidson NO, Isolation, characterization and developmental regulation of the human apobec-1 complementation factor (ACF) gene. Biochim Biophys Acta, 2001. 1522(1): p. 22–30. [PubMed: 11718896]
13. Lellek H, et al. , Purification and molecular cloning of a novel essential component of the apolipoprotein B mRNA editing enzyme-complex. J Biol Chem, 2000. 275(26): p. 19848–56. [PubMed: 10781591]

14. Fossat N, et al. , C to U RNA editing mediated by APOBEC1 requires RNA-binding protein RBM47. EMBO Rep, 2014. 15(8): p. 903–10. [PubMed: 24916387]
15. Blanc V, et al. , Apobec1 complementation factor (A1CF) and RBM47 interact in tissue-specific regulation of C to U RNA editing in mouse intestine and liver. RNA, 2019. 25(1): p. 70–81. [PubMed: 30309881]
16. Lerner T, Papavasiliou FN, and Pecori R, RNA Editors, Cofactors, and mRNA Targets: An Overview of the C-to-U RNA Editing Machinery and Its Implication in Human Disease. Genes, 2019. 10(1): p. 13.
17. Burd CG and Dreyfuss G, Conserved structures and diversity of functions of RNA-binding proteins. Science, 1994. 265(5172): p. 615–21. [PubMed: 8036511]
18. Lin J, et al. , Abstract 18960: RNA-binding Protein A1CF Modulates Plasma Triglyceride Levels Through Transcriptomic Regulation of Stress-Induced VLDL Secretion. Circulation, 2017. 136(suppl_1): p. A18960–A18960.
19. Kim YE, et al. , RBM47-regulated alternative splicing of TJP1 promotes actin stress fiber assembly during epithelial-to-mesenchymal transition. Oncogene, 2019. 38(38): p. 6521–6536. [PubMed: 31358901]
20. Radine C, et al. , The RNA-binding protein RBM47 is a novel regulator of cell fate decisions by transcriptionally controlling the p53-p21-axis. Cell Death Differ, 2020. 27(4): p. 1274–1285. [PubMed: 31511650]
21. Wolfe AD, Arnold DB, and Chen XS, Comparison of RNA Editing Activity of APOBEC1-A1CF and APOBEC1-RBM47 Complexes Reconstituted in HEK293T Cells. J Mol Biol, 2019. 431(7): p. 1506–1517. [PubMed: 30844405]
22. Blanc V, et al. , Identification of GRY-RBP as an apolipoprotein B RNA-binding protein that interacts with both apobec-1 and apobec-1 complementation factor to modulate C to U editing. J Biol Chem, 2001. 276(13): p. 10272–83. [PubMed: 11134005]
23. Rosenberg BR, et al. , Transcriptome-wide sequencing reveals numerous APOBEC1 mRNA-editing targets in transcript 3' UTRs. Nat Struct Mol Biol, 2011. 18(2): p. 230–6. [PubMed: 21258325]
24. Kankowski S, et al. , A Novel RNA Editing Sensor Tool and a Specific Agonist Determine Neuronal Protein Expression of RNA-Edited Glycine Receptors and Identify a Genomic APOBEC1 Dimorphism as a New Genetic Risk Factor of Epilepsy. Front Mol Neurosci, 2017. 10: p. 439. [PubMed: 29375302]
25. Nelson VR, et al. , Transgenerational epigenetic effects of the Apobec1 cytidine deaminase deficiency on testicular germ cell tumor susceptibility and embryonic viability. Proceedings of the National Academy of Sciences, 2012. 109(41): p. E2766–E2773.
26. Cole DC, et al. , Loss of APOBEC1 RNA-editing function in microglia exacerbates age-related CNS pathophysiology. Proceedings of the National Academy of Sciences, 2017. 114(50): p. 13272–13277.
27. Gout JF, et al. , The landscape of transcription errors in eukaryotic cells. Sci Adv, 2017. 3(10): p. e1701484. [PubMed: 29062891]
28. Kim K, et al. , The roles of APOBEC-mediated RNA editing in SARS-CoV-2 mutations, replication and fitness. Sci Rep, 2022. 12(1): p. 14972. [PubMed: 36100631]
29. Liu Z, et al. , Systematic comparison of 2A peptides for cloning multi-genes in a polycistronic vector. Scientific reports, 2017. 7(1): p. 1–9. [PubMed: 28127051]
30. Chen Z, Eggerman TL, and Patterson AP, ApoB mRNA editing is mediated by a coordinated modulation of multiple apoB mRNA editing enzyme components. American Journal of Physiology-Gastrointestinal and Liver Physiology, 2007. 292(1): p. G53–G65. [PubMed: 16920700]
31. Snyder EM, et al. , APOBEC1 complementation factor (A1CF) is dispensable for C-to-U RNA editing in vivo. Rna, 2017. 23(4): p. 457–465. [PubMed: 28069890]
32. Blanc V, et al. , Genome-wide identification and functional analysis of Apobec-1-mediated C-to-U RNA editing in mouse small intestine and liver. Genome Biol, 2014. 15(6): p. R79. [PubMed: 24946870]

33. Grunewald J, et al. , Transcriptome-wide off-target RNA editing induced by CRISPR-guided DNA base editors. Nature, 2019. 569(7756): p. 433–437. [PubMed: 30995674]

34. Mehta A and Driscoll DM, Identification of domains in apobec-1 complementation factor required for RNA binding and apolipoprotein-B mRNA editing. Rna, 2002. 8(1): p. 69–82. [PubMed: 11871661]

35. Blanc V, Henderson JO, Kennedy S, and Davidson NO, Mutagenesis of apobec-1 complementation factor reveals distinct domains that modulate RNA binding, protein-protein interaction with apobec-1, and complementation of C to U RNA-editing activity. Journal of Biological Chemistry, 2001. 276(49): p. 46386–46393. [PubMed: 11571303]

36. Malhotra S and Sowdhamini R, Sequence search and analysis of gene products containing RNA recognition motifs in the human genome. BMC Genomics, 2014. 15(1): p. 1159. [PubMed: 25534245]

37. Sowden M, Hamm JK, and Smith HC, Overexpression of APOBEC-1 Results in Mooring Sequence-dependent Promiscuous RNA Editing (*). Journal of Biological Chemistry, 1996. 271(6): p. 3011–3017. [PubMed: 8621694]

38. Wolfe AD, Li S, Goedderz C, and Chen XS, The structure of APOBEC1 and insights into its RNA and DNA substrate selectivity. NAR Cancer, 2020. 2(4): p. zcaa027.

39. Schneider CA, Rasband WS, and Eliceiri KW, NIH Image to ImageJ: 25 years of image analysis. Nat Methods, 2012. 9(7): p. 671–5. [PubMed: 22930834]

40. Crooks GE, Hon G, Chandonia JM, and Brenner SE, WebLogo: a sequence logo generator. Genome Res, 2004. 14(6): p. 1188–90. [PubMed: 15173120]

Highlights

- RBM46 (RNA-binding-motif-protein-46) is a novel A1 cofactor identified for RNA editing.
- RRM2 and RRM3 domains are essential for RBM46 function in complementing A1 RNA editing activity.
- Some cellular RNA targets in HEK293 cells for A1+RBM46 editing are identified using the low-error circular RNAseq technique.
- RNA containing an AAA motif from −3’ to −5’ positions of the target-C shows increased editing efficiency by A1+RBM46.

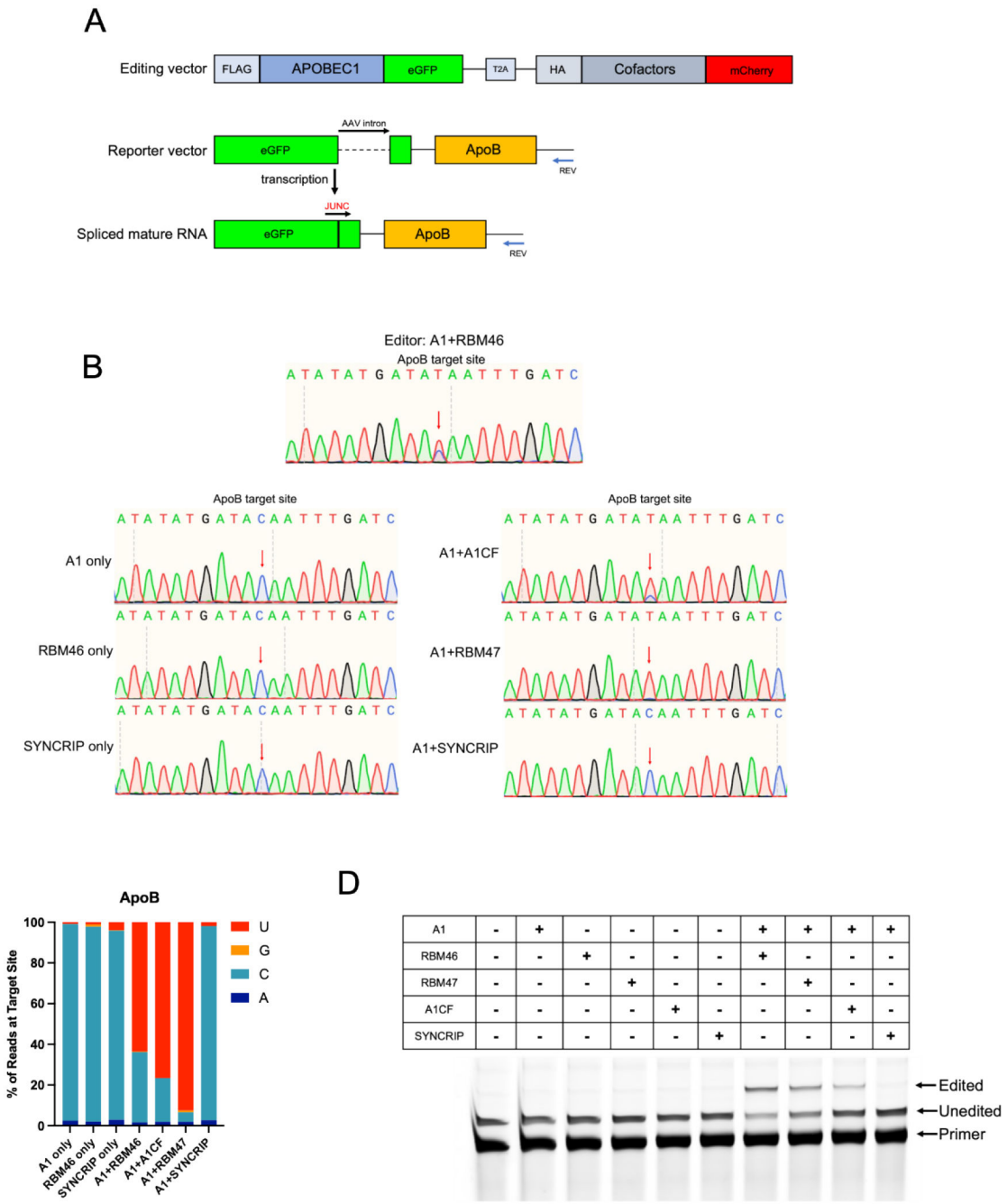

Figure 1: A1+RBM46 showed editing activity on ApoB RNA.

(A). Cartoon depiction of the reporter and editor constructs used in this study. The editor construct expresses FLAG-A1, a cofactor (HA-A1CF, HA-RBM46, HA-RBM47 or HA-SYNCRIP), and mCherry as individual, cleaved proteins from a single open reading frame via self-cleaving 2A peptides. For the reporter construct, an AAV intron is inserted with the eGFP fusion protein to ensure only mature RNA is sequenced, and a target RNA substrate transcript sequence is inserted. Shown here is the minimal 33-base ApoB target RNA transcript sequence known to be edited by A1 in the presence of a cofactor. **(B).** Sanger sequencing trace file shows that A1+RBM46, A1+A1CF, and A1+RBM47 can all edit ApoB

RNA from AC to AT, but A1+SYNCRIP, A1, RBM47, and SYNCRIP alone cannot. After transfection of the editor and reporter into HEK293T cells, ApoB RNA was purified and amplified by the specific primer for Sanger sequencing. Each A,T, C, G read number is calculated. **(C).** Comparison of A1 and different cofactors editing activity on ApoB RNA.

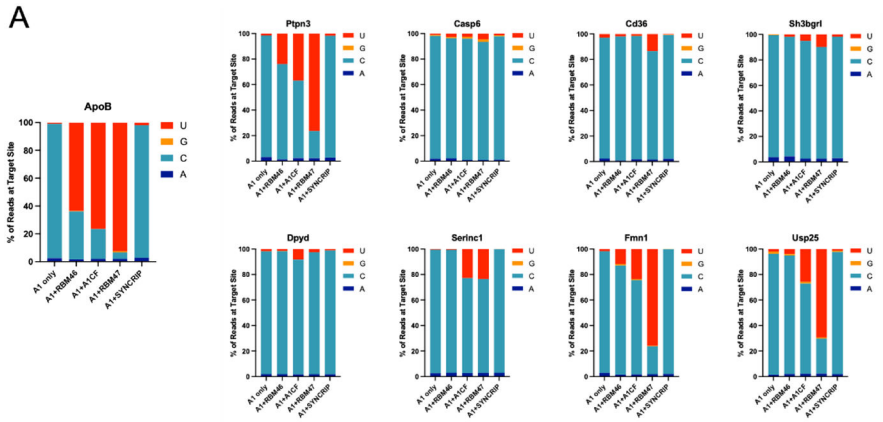

B

	ApoB	Ptpn3	Casp6	Cd36	Sh3bgrl	Dpyd	Serinc1	Fmn1	Usp25
A1 only	0.97	1.70	1.07	2.90	0.14	1.68	0.52	1.80	2.07
A1+RBM46	63.60	24.04	2.76	1.96	1.82	1.49	0.58	11.95	4.06
A1+A1CF	76.59	36.95	2.58	1.53	5.28	8.35	22.82	23.71	25.79
A1+RBM47	92.54	76.52	4.55	13.53	9.94	2.52	23.56	75.93	69.46
A1+SYNCRIP	1.90	1.84	1.26	0.63	1.79	1.18	0.24	0.00	1.28

% of U at target C site: 100, 80, 60, 40, 20, 0

C

ApoB_48 nt
5′ – UCUCAACUGCAGACAUAUAUGAUACAAUUUGAUCAGUAUAUUAAAGAU – 3′

ApoB_96nt
5′-AAAAUCAACUUUAAUGAAAAACUAUCUCAACUGCAGACAUAUAUGAUACAAUUUGAUCAGUAUAUUAAAGAUAGUUAUGAUUUACAUGAUUUGAAA – 3′

Ptpn3: 48 nt
5′ –UGUUGUCGGAACUCUACUGAAAAACAACCUGAUCAAUAUAAAAGCGUU– 3′

Ptpn3_96nt
5′ –UGUAAAUUUGGAAUGUUUUCUCAUCCUGACUUGUUGUCGGAACUCUACUGAAAAACAACCUGAUCAAUAUAAAAGCGUUCAAGCUAUGCAACACUG – 3′

D

	A1 only	A1+RBM46	A1+A1CF	A1+RBM47	A1+SYNCRIP
ApoB_48nt	3.16	72.22	84.82	92.02	4.53
ApoB_96nt	7.03	87.73	92.98	91.88	10.52
Ptpn3_48nt	0.98	23.92	56.72	75.90	2.37
Ptpn3_96nt	1.37	34.79	70.00	85.94	4.02

% of U at target C site: 100, 80, 60, 40, 20

Figure 2. Comparison of editing activities on a set of identified RNA substrates by the human A1 and its different cofactors (RBM46, A1CF, RBM47, and SYNCRIP).

(A). Quantification of editing on different RNA targets by counting the number of A, C, G, U reads at target C position of Sanger Sequencing results. (B). Heat map shows the calculated percentage of U at targeted C sites. A1 and SYNCRIP did not show editing activity on any tested substrates. (C). Sequence of ApoB and Ptpn3 with 48nt and extended 96nt for the comparison of side-by-side editing assay. (D). Heat map shows the calculated percentage of U at targeted C sites of Sanger Sequencing results.

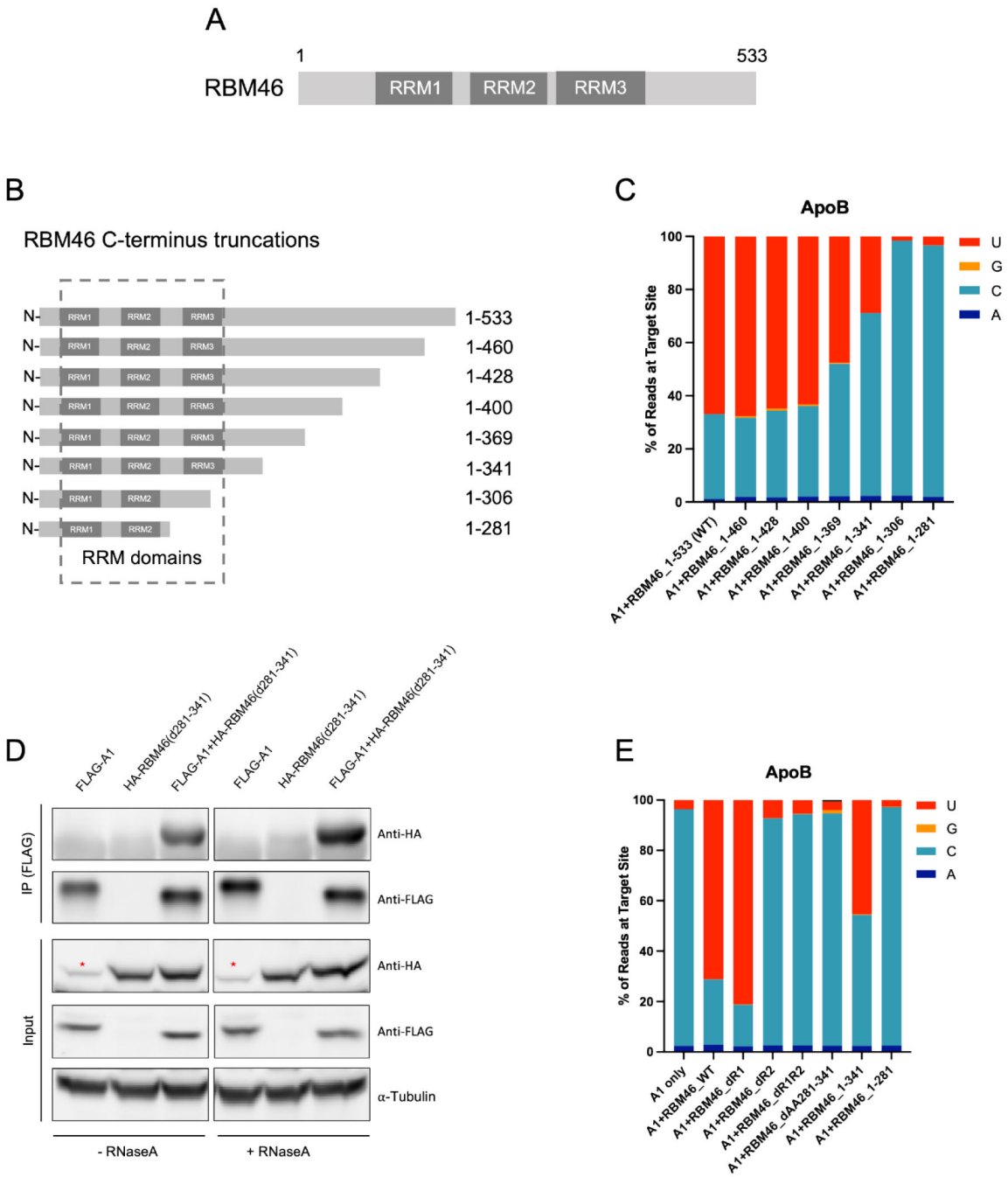

Figure 3. Identification of RBM46 domains required for A1+RBM46 RNA editing activity.

(A). Cartoon showing RBM46 protein domain structure. RRM: RNA recognition motif. (B). RBM46 C-terminal truncation constructs. The three RRM domains are indicated by dashed-line box. (C). The editing assay result of A1 plus the various RBM46 deletion constructs indicates that RBM46's activity started to decrease when the C-terminus is shortened beyond residue 400, and no activity was present when part of the RRM domain is deleted (1–306), indicating the importance of the three RRM for its complementary activity for A1 deamination. (D). Co-immunoprecipitation data of A1 and RBM46 with deletion

of amino acid 281–341 using the anti-FLAG beads followed by western blot. Anti-HA, anti-FLAG, and anti-Tubulin primary antibodies are used in western blot, showing that A1 has interaction with RBM46(d281–341). The red star indicates the lane for uncleaved FLAG-A1-F2A-mCherry. (E). The editing assay result of A1 plus the various RBM46 RRM-deletion constructs indicates that RBM46 RRM1 is the only dispensable RRM for its complementary activity for A1 deamination.

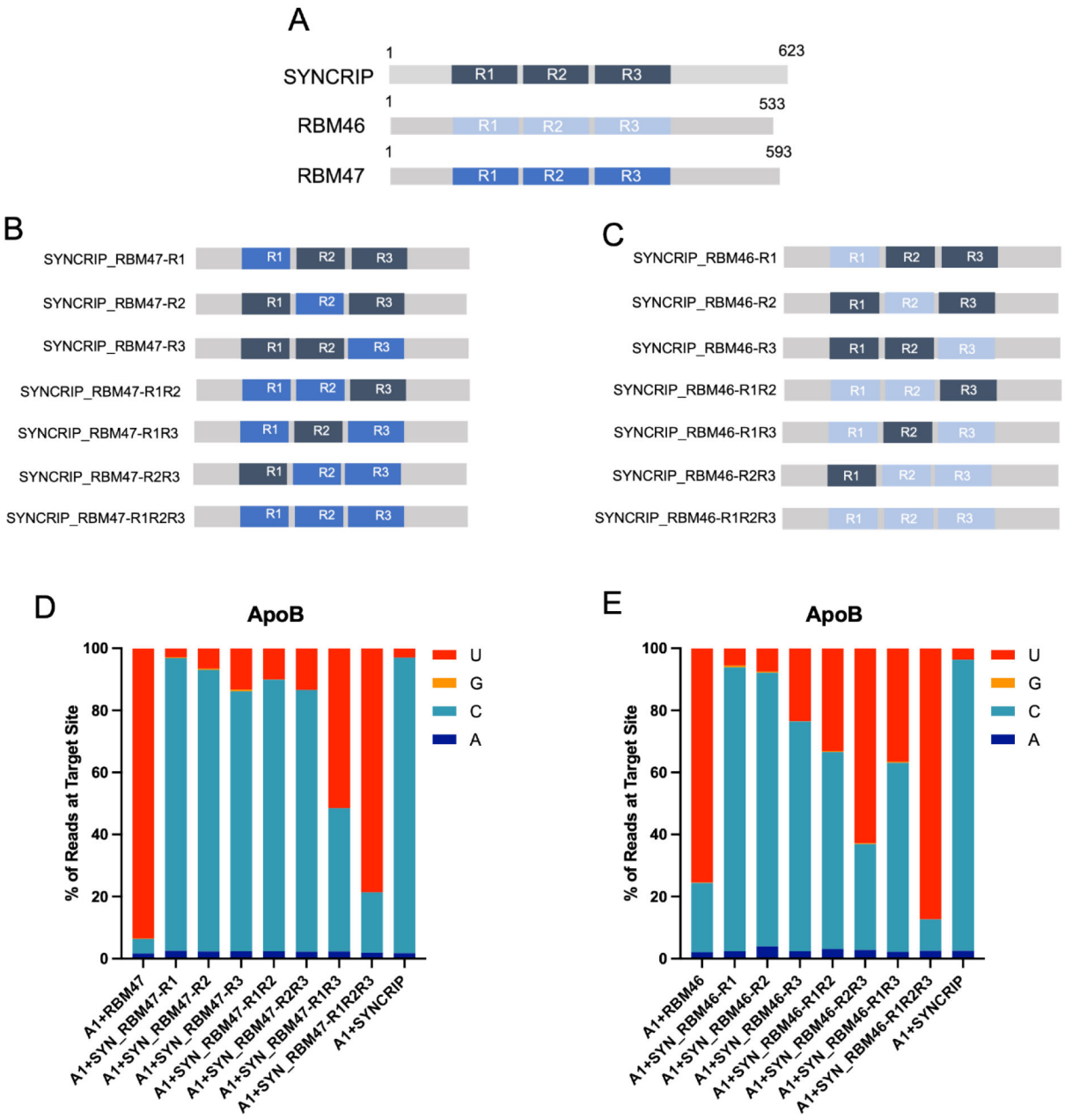

Figure 4. The activity of SYNCRIP-chimeras containing RRMs from RBM46/47 on complementing A1 RNA editing.

(A). Cartoon showing domain structures of SYNCRIP, RBM46, and RBM47, all of which contain three homologous RRM domains (RNA recognition motif, R1, R2, R3). SYNCRIP cannot complement A1 RNA editing activity. **(B).** The SYNCRIP-RBM47 chimera design. The three SYNCRIP RRM domains were replaced individually or in different combinations with the three RBM47 RRMs on the SYNCRIP clone. Now the editor construct contains FLAG-A1 (not shown in the figure) and HA-SYNCRIP-RBM47 chimeras. **(C)**. The SYNCRIP-RBM46 chimera design. The three SYNCRIP RRM domains were replaced individually or in different combinations with the three RBM46 RRMs on the SYNCRIP clone. **(D)**. The editing result on ApoB RNA in the presence of A1+SYNCRIP-RBM47

chimera. Each of the three RBM47 RRMs in SYNCRIP-RBM47 chimera showed some levels of RNA editing activity with A1 individually, and combinations of R1, R2, and R3 showed synergistic effect on editing activity. (E). Each of the three RBM46 RRMs in SYNCRIP-RBM46 chimera showed some levels of RNA editing activity with A1 individually, and combinations of R1, R2, and R3 showed synergistic effect on editing activity.

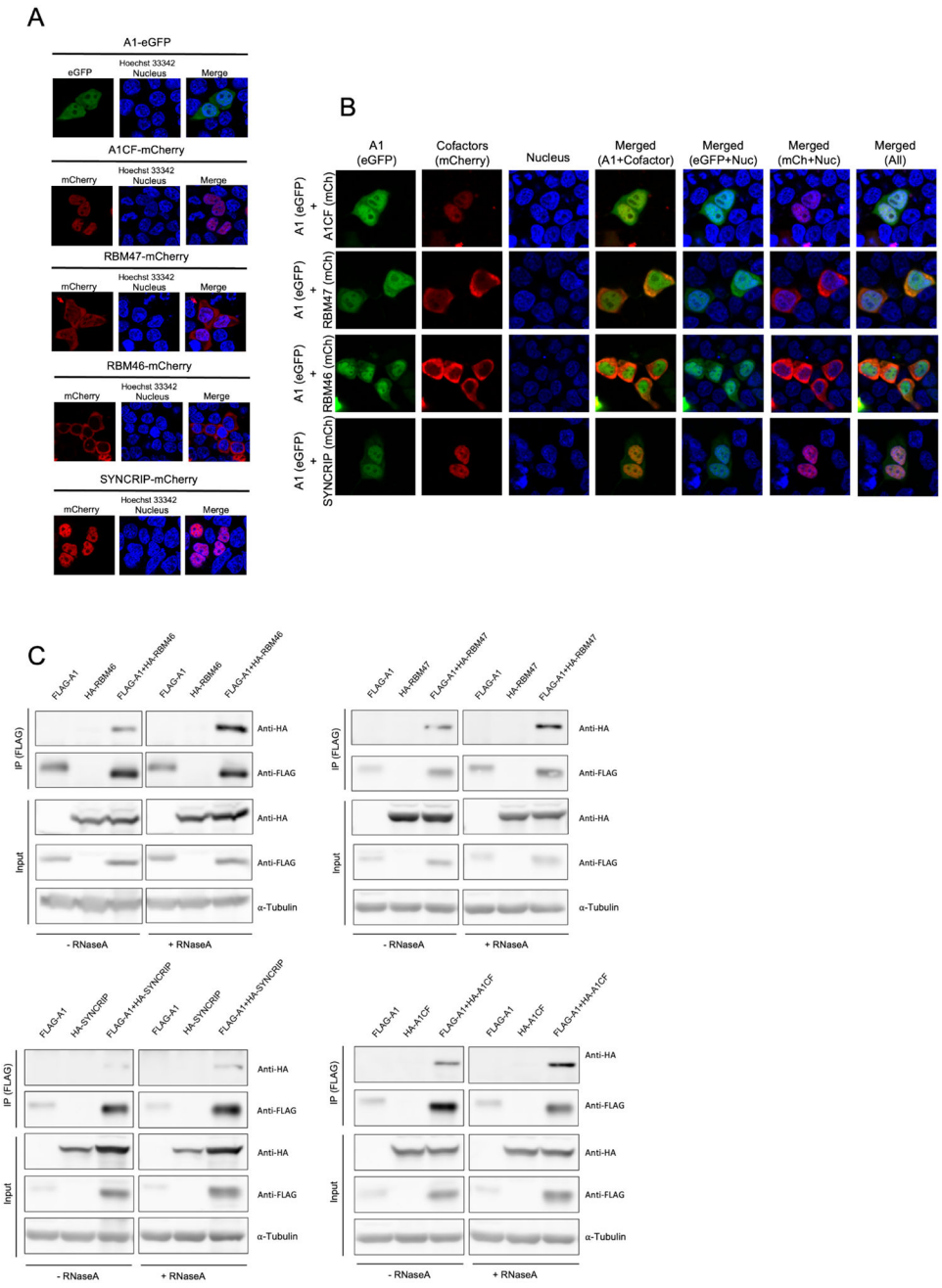

Figure 5. Fluorescence localization data of A1-eGFP (green), cofactors-mCherry (red), and co-immunoprecipitation data of A1 with its cofactors.

(A). Overexpression of A1-eGFP and cofactors-mCherry alone in HEK293T cells show subcellular localization. The nucleus is stained by Hoechst 33342 (Blue). **(B).** All cofactors co-expressed with A1, showing the colocalization pattern in HEK293T cells. **(C).** Co-immunoprecipitation result of A1 and cofactors (RBM46, RBM47, A1CF, and SYNCRIP) using the anti-FLAG beads followed by western blot. Anti-HA-cofactor, anti-FLAG-A1, and anti-Tubulin primary antibodies are used in western blot, showing that A1 has interactions with all cofactors (RBM46, RBM47, A1CF, and SYNCRIP).

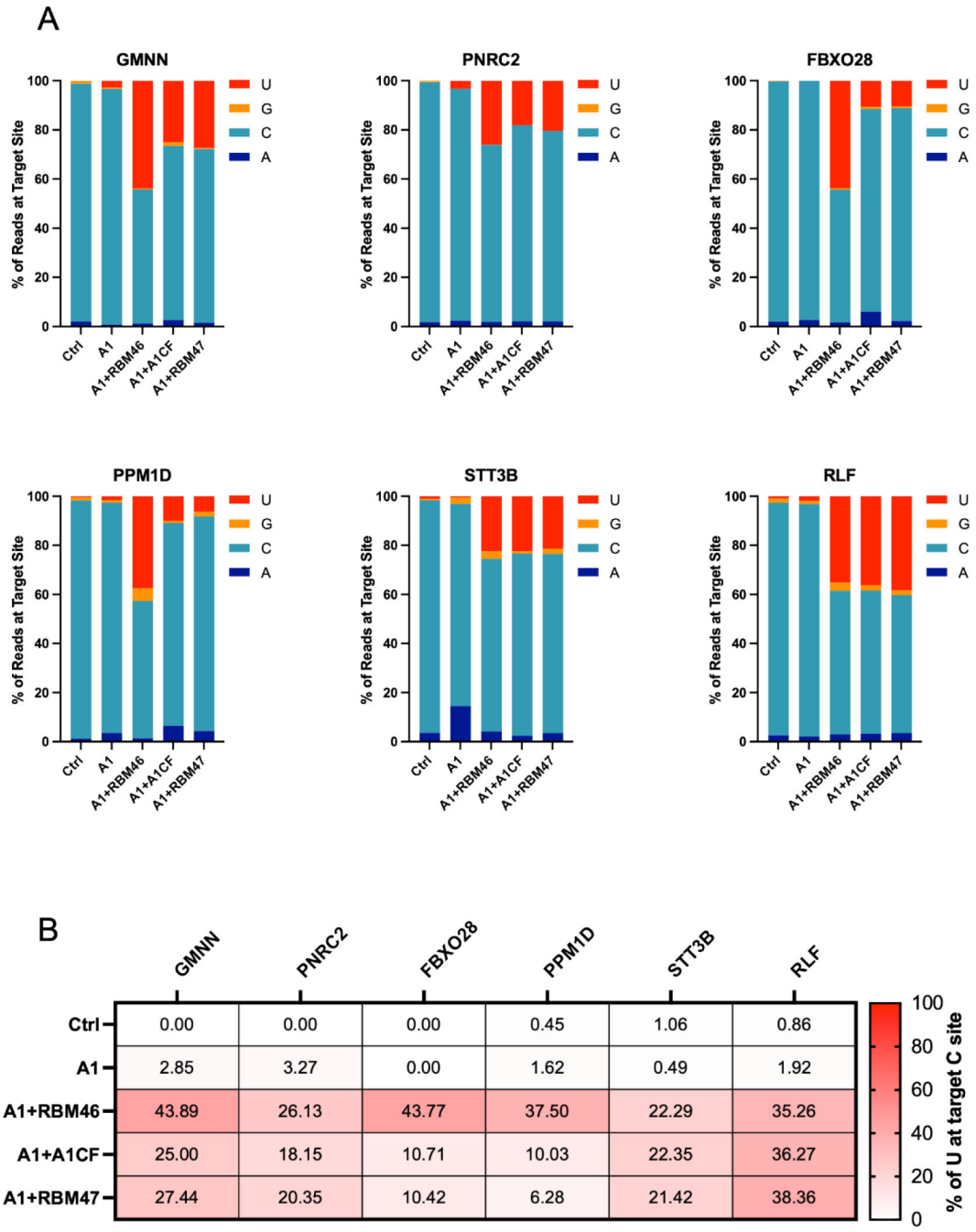

Figure 6. Validation of selected A1/RBM46 RNA target from Circular RNA seq by Sanger Sequencing with A1/cofactors over-expression in HEK293T cell.

(A). Quantification of editing on different selected RNA targets by counting the number of A, C, G, U reads at target C position of Sanger Sequencing results. A1/cofactors editors are transfected into HEK293T cell. The cDNA is synthesized by designed reverse primer. PCR is applied to amplify the cDNA for Sanger Sequencing. (B). Heat map shows the calculated percentage of U at targeted C sites. All cofactors paired with A1 show editing activities on the selected RNA target. A1/RBM46 shows higher editing level on GMNN, FBX028, PPM1D target.

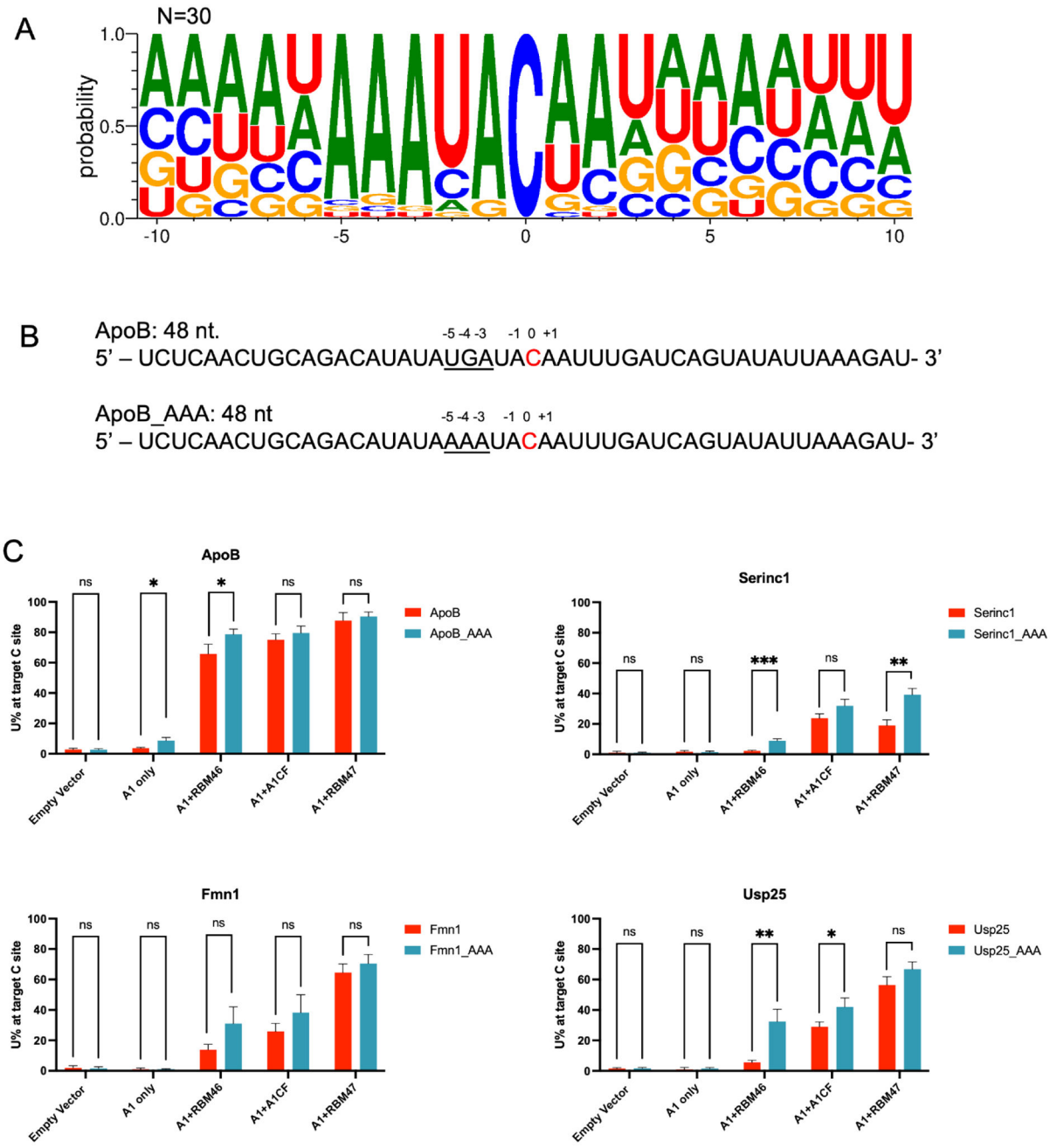

Figure 7. The effects of AAA motif at −3, −4, −5 position of RNA substrates on the editing activity for A1 paired with RBM46 and other cofactors.

(A). Local sequences around the significantly edited target C sites (± 10 nucleotides from target C at position 0) of RNA targets from table 1 (n=30). **(B).** Original ApoB RNA sequence contained in the reporter vector and the ApoB RNA sequence with the change of AAA motif at −3, −4, −5 position. **(C).** Comparison of the C-to-U editing rates on defined original A1 RNA targets (red bar) and the modified RNA targets with AAA at −3, −4, −5 position (blue bar) by different A1 editosomes. The statistical significance was calculated

by unpaired two-tailed t-test with *P*-values represented as: P > 0.05 = not significant; not indicated, *P < 0.05, ***P < 0.001, ****P < 0.0001.

Table 1:

APOBEC1 and RBM46 RNA targets identified from Circular RNA Seq (>=30% editing efficiency)

	RNA	Chr	Position	Reference base	C-RNA seq
1	GMNN	6	24785950 (+)	AAATA**C**TATG	66.67%
2	PNRC2	1	23962463 (+)	AAATA**C**ACCA	60.00%
3	CEBPZ	2	37220451 (−)	GGATC**G**TATTT	58.33%
4	TULP3	12	2939639 (+)	AAACA**C**ACAC	57.14%
5	AZIN1	8	102828449 (−)	TAATA**G**TTTTT	54.55%
6	FBXO28	1	224161584 (+)	AAATA**C**TAAA	50.00%
7	PPP6C	9	125149755 (−)	CTCTT**G**TATTT	50.00%
8	SMNDC1	10	110294177 (−)	ACATT**G**TATTT	48.15%
9	PPM1D	17	60664151 (+)	AAATA**C**TATG	45.45%
10	TRIP12	2	229791150 (−)	TTTTT**G**CATTT	45.45%
11	FBXO5	6	152975184 (−)	GCTTT**G**TATTT	44.00%
12	PITPNA	17	1519920 (−)	TACTC**G**TATTT	41.18%
13	HMGB1	13	30460909 (−)	AAATT**G**TATTT	40.00%
14	KAT2A	17	42114921 (−)	GGACA**G**CTCCG	38.89%
15	STT3B	3	31636468 (+)	AAATA**C**AAGT	35.71%
16	LMAN1	18	59330743 (−)	CAAGT**G**TGTTT	33.33%
17	ID2	2	8684398 (+)	AAATA**C**AAGT	33.33%
18	TRAPPC8	18	31916313 (−)	ACATA**G**TATTT	31.82%
19	SIKE1	1	114773539 (−)	TTTTA**G**TATTT	31.58%
20	PITPNB	22	27852859 (−)	GTCTA**G**TATTT	31.25%
21	H2AC18	1	149842299 (−)	CGGAC**G**TCAGC	30.92%
22	ODR4	1	186390847 (+)	AAATA**C**AAAG	30.77%
23	TMEM123	11	102397921 (−)	TAGGT**G**TGTTT	30.77%
24	PPP4R3B	2	55548714 (−)	AAATT**G**TATTT	30.77%
25	BCLAF1	6	136259379 (−)	TTATG**G**TATTT	30.77%
26	NCOA4	10	46005206 (−)	ACAGT**G**TGTTT	30.30%
27	RLF	1	40238258 (+)	AAACA**C**ACCT	30.00%
28	SLC38A1	12	46188638 (−)	TTATT**G**TATAT	30.00%

(+) Sense strand.

(−) Antisense strand.